A Block Supramolecular Polymer and Its Kinetically Enhanced Stability

A Block Supramolecular Polymer and Its Kinetically Enhanced Stability

Sung Ho Jung,[†] Davide Bochicchio,[‡] Giovanni M. Pavan,*[,‡] Masayuki Takeuchi1,*[, †] Kazunori Sugiyasu*[, †]

[†] National Institute for Materials Science (NIMS), 1-2-1 Sengen, Tsukuba, Ibaraki 305-0047, Japan

[‡]Department of Innovative Technologies, University of Applied Sciences and Arts of Southern Switzerland, CH-6928 Manno, Switzerland

ABSTRACT: Biomolecular systems serve as an inspiration for the creation of multicomponent synthetic supramolecular systems that can be utilized to develop functional materials with complexity. However, supramolecular systems rapidly reach an equilibrium state through dynamic and reversible non-covalent bonds, resulting in a disorganized mixture of components rather than a system in which individual components function cooperatively and/or independently. Thus, efficient synthetic strategies and characterization methods for intricate multicomponent supramolecular assemblies need to be developed. Herein, we report the synthesis of porphyrin-based supramolecular polymers (SPs) in which two distinct block segments consisting of different metal porphyrins are connected: i.e., block supramolecular polymers (BSPs). BSPs with a controlled length and narrow polydispersity were achieved through seeded-growth by a solvent mixing protocol. Interestingly, the block structure permitted the SP as an inner block to coexist with a reagent that was otherwise incompatible with the SP alone. We infer that the inner SP block is compartmentalized in the block structure and endowed with the kinetic stability. Molecular simulations revealed that monomer exchange occurs from the termini of the SP, which corroborated the enhanced stability of the BSP. These results are expected to pave the way for the design of more complex multicomponent supramolecular systems.

INTRODUCTION

In the light of the substantial contribution of living polymerization to polymer science[1,2], the recent development of its supramolecular counterpart, i.e., living supramolecular polymerization[3,4], has inspired us to expand the scope of molecular self-assembly in the fields of materials science, nanotechnology, and biotechnology[5-7]. In this regard, the synthesis of block supramolecular polymers (BSPs), which offers unprecedented structural complexity and sophisticated functionality, has attracted considerable attention despite it being significantly challenging[8].

Based on the previous studies[9-25], we infer the prerequisites of living supramolecular polymerization and the issues associated with the synthesis of BSPs. First, the nucleation–elongation mechanism[26-29] should be operative so that supramolecular polymerization can be processed in a manner analogous to chain growth polymerization. In general, such supramolecular polymers (SPs) have high degrees of internal order (or crystallinity); accordingly, the synthesis of BSPs appears as difficult as welding two single crystals of different molecules. To this end, it is necessary to consider interfacial design between the two blocks, including intermolecular interactions and lattice matching[30]. Second, a metastable state has to be involved such that an otherwise spontaneous nucleation process is kinetically suppressed. Formation of a competing aggregate[9,10] and intramonomer hydrogen-bonding[11-14,20,21] have been demonstrated to be effective for this purpose. However, it is still difficult to manage the pathway complexity because the delicate balance between the stabilities of the metastable species and SPs gets readily disrupted if the monomer structure is altered[10,13,31]. Given the abovementioned considerations, monomer design of the second block in a BSP is inevitably restricted by the monomer structure of the first block.

One-dimensional (1D) block nanostructures have been reported to date[8,32-40], and in particular, living crystallization-driven self-assembly (CDSA) has been demonstrated to be a powerful method to obtain such architectures via self-assembly[34-37]. Nevertheless, 1D block nanostructures with a *unimolecular* width (i.e., BSPs) are quite rare[8,10,15,17]. Previously, van der Gucht, Otto, and co-workers[15] synthesized a BSP of peptide-based macrocyclic monomers bearing *benzyl* and *cyclohexylmethyl* side chains. We have also achieved a BSP of porphyrin monomers bearing *methoxy* (**2$_{Zn}$Me**) and *hexyloxy* (**2$_{Zn}$Hex**) side chains (Figure 1)[10]. These examples imply that monomer structures in a BSP have to be very similar, which corroborates the aforementioned assertion. In fact, regarding our previous porphyrin systems, even a BSP consisting of different metal porphyrin cores (e.g., **2$_{Zn}$Me** and **2$_{Cu}$Me**) could not be obtained (S. Ogi, M. Takeuchi,

K. Sugiyasu, unpublished results). Although Palmans, Meijer, and co-workers recently reported characterization of BSPs under thermodynamic control[8], the functions and properties of BSPs arising from dissimilar SP blocks have thus far been virtually unexplored.

Herein, we assessed the applicability of the living CDSA method to the synthesis of unimolecular BSPs. In this protocol, seeded-growth is performed by mixing good and poor solvents for monomers. Manners and co-workers extended their living CDSA method to the supramolecular polymerization of platinum complexes and succeeded in controlling the length of SPs[16,17]. Furthermore, they succeeded in creating a unique scarf-like nanostructure consisting of the platinum complexes bearing polyethylene glycol side chains with different lengths (i.e., $(C_2H_4O)_n$, where n = 12 or 16)[17]. For the synthesis of BSPs, de Greef, Meijer, and co-worker[41] proposed a stepwise assembly of multicomponent structures by using good and poor solvents based on their in-depth mechanistic study; however, this strategy has not been attempted as yet.

We succeeded in connecting the SPs consisting of distinct porphyrin cores in B–A–B type triblock copolymer structures through the solvent mixing protocol. Interestingly, it was found that the stability of block A could be kinetically enhanced by the presence of block B, which illustrates a collective property of BSPs dictated by the block sequence. This study represents an important step toward the synthesis of advanced multicomponent SPs that have been increasingly attracting attention in recent years[42-47].

RESULTS AND DISCUSSION

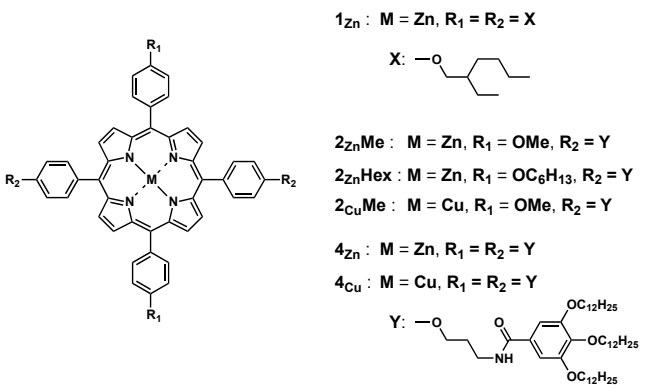

Figure 1. Structure of porphyrin-based monomers.

Molecular design. As mentioned above, BSPs of different metal porphyrin monomers could not be obtained in our previous study (e.g., by using **2ZnMe** and **2CuMe**) because these monomers showed different self-assembling behavior (Figures S5 and S6 for **2ZnMe** and **2CuMe**, respectively). We reasoned that these porphyrin cores are distorted differently and adopt different stacking modes[48]. To address this issue, we increased the number of hydrogen bonding sites so that the junction between the different metal porphyrin cores could be matched and stabilized. The synthesis and characterization of the new monomers, namely, **4Zn** and **4Cu**, (Figure 1), are described in the Supporting Information.

Supramolecular polymerization. As discussed later, seeded-growth in living CDSA is typically performed in a mixed solvent system. In this study, a mixture of methylcyclohexane (MCH): a poor solvent that induces self-assembly of porphyrin monomers, and toluene: a good solvent in which porphyrin monomers are molecularly dissolved, was used. Figure 2 illustrates the supramolecular polymerization of the zinc(II)-porphyrin monomer (**4Zn**) in mixed solvents.

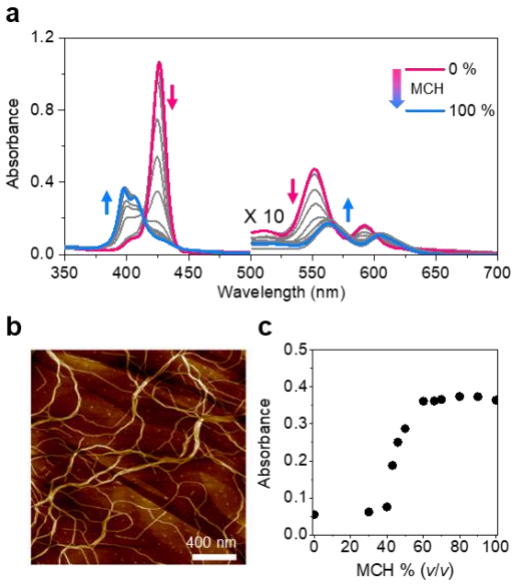

Figure 2. Self-assembling behavior of **4Zn** in MCH/toluene mixed solvents. (a) Absorption spectra of **4Zn** in MCH/toluene mixed solvents: [**4Zn**] = 10 μM. (b) AFM image of supramolecular polymer of **4Zn** (i.e., SP**4Zn**) prepared in MCH/toluene (2:1) mixed solvent: scale bar, 400 nm. (c) Plot of absorbance at 398 nm as a function of MCH proportion.

On increasing the proportion of MCH, the Soret band blue-shifted (Figure 2a), which suggested that the porphyrin chromophores were self-assembled in a face-to-face stacking manner, i.e., H aggregate mode[9,10]. Atomic force microscopy (AFM) visualized the 1D supramolecular polymer (Figure 2b). The plot of absorbance at 398 nm as a function of the proportion of MCH showed a critical MCH/toluene ratio as ~40% of MCH, below which complete disassembly occurs (Figure 2c). This result implied that supramolecular polymerization of **4Zn** proceeded via the nucleation–elongation mechanism[41,49,50]. In fact, temperature-dependent absorption spectral changes (cooling process) accompanied a critical elongation temperature (T_e), a characteristic of the nucleation–elongation process (Figure 3a,b)[51-53]. We found a linear relationship between the T_e values and the proportion of MCH (Figure 3c).

Figure 3b shows the temperature-dependent degree of supramolecular polymerization obtained for solutions of **4Zn**; the results obtained for 67% MCH solution are

shown as typical cooling curves. The elongation regime, i.e., the curve below T_e, could be fitted by the model developed by van der Shoot and Meijer[51]. The elongation enthalpy (H_e) determined from curve fitting was –108 kJ mol^{-1} for the curve of [**4**$_{Zn}$] = 10 μM. The standard enthalpy ($\Delta H°$) and entropy ($\Delta S°$) for the elongation process were determined from a van't Hoff plot to be –119 kJ mol^{-1} and –271 J mol^{-1} K^{-1}, respectively (Figure S7). Thus, the Gibbs free energy ($\Delta G°$) at 298 K was calculated to be –38 kJ mol^{-1}. Likewise, 1D supramolecular polymerization of **4**$_{Cu}$ was assessed (Figures S9 and S10): $\Delta H°$ = –122 kJ mol^{-1}, $\Delta S°$ = –284 J mol^{-1} K^{-1}, and $\Delta G°$ (at 298 K) = –37 kJ mol^{-1}.

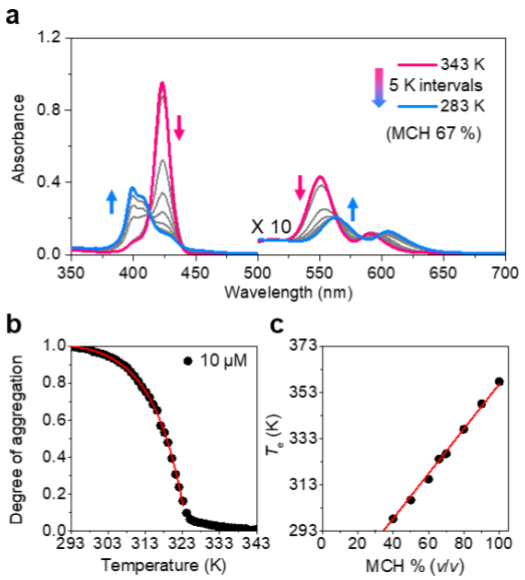

Figure 3. Supramolecular polymerization of **4**$_{Zn}$ in MCH/toluene (2:1). (a) Temperature-dependent absorption spectral changes of **4**$_{Zn}$ in MCH/toluene (2:1): [**4**$_{Zn}$] = 10 μM. (b) Changes in the degrees of supramolecular polymerization (α) of **4**$_{Zn}$ in MCH/toluene (2:1) as a function of temperature. A red solid line is the fitting curve for [**4**$_{Zn}$] = 10 μM, obtained from cooperative model. (c) Plot of T_e values as a function of MCH proportion.

As demonstrated above, the new porphyrin monomers (**4**$_{Zn}$ and **4**$_{Cu}$) have a strong propensity for supramolecular polymerization because of the increased number of hydrogen-bonding sites. Thus, it is anticipated that block junction between dissimilar SPs could be stabilized to produce BSPs. However, unlike our previous system of **2**$_{Zn}$**Me**[9,10], the supramolecular polymerization of these new monomers does not involve a metastable state, which eliminated the possibility of kinetic control over supramolecular polymerization (see the prerequisites discussed in the Introduction). As such, a dilemma was inherent in this monomer design, which led us to investigate whether the solvent mixing protocol such as the living CDSA was applicable to the synthesis of unimolecular BSPs[16,17].

Living supramolecular polymerization. Figure 4a depicts the scheme of living supramolecular polymerization performed in this study. Briefly, solutions of the seeds of a SP (in MCH) and a monomer (in toluene) were mixed to initiate the seeded-growth. The plots of the temperatures at which the degree of aggregation reached 97% against the proportion of MCH suggested that **4**$_{Zn}$ is fully dissolved in toluene but self-assembles in 67 % MCH at 298 K ([**4**$_{Zn}$] = 10 μM, Figure S11). Therefore, provided a sufficiently high monomer concentration, this plot assures that a high degree of aggregation (>95%) can be retained when the solutions of the seeds (in MCH) and the monomer (in toluene) are mixed in a ratio of 2 to 1 at 298 K (i.e., 67% MCH); this mixing ratio is used for the experiments that follow.

The scheme shown in Figure 4a requires seeds of a SP. By sonication (90 W at 2 °C for 3 h), SP**4**$_{Zn}$ fragmented into short pieces with the number average length (L_n) and weight average length (L_w) of 86 and 102 nm, respectively (Figure 4b. Figures S12a-c). The absorption spectrum of these SP**4**$_{Zn}$ seeds was identical to that of SP**4**$_{Zn}$, indicating that the H aggregate mode was preserved (Figure S12d).

The MCH solution of SP**4**$_{Zn}$ seeds was placed carefully on the top of the toluene solution of monomeric **4**$_{Zn}$ in a cuvette, which was then shaken for a few seconds at room temperature (Figure S13). The color of the mixed solution instantaneously changed to that of the H aggregate. The kinetics of the seeded-growth was too fast to be monitored even with the stopped-flow setup. The "depolymerization overshoot"[41] of the seed—the temporal depolymerization caused by inefficient mixing of the good and poor solvents—was not observed in both the manual mixing experiment and the stopped-flow experiment (Figure S14).

Figures 4c and d show the AFM images of SP**4**$_{Zn}$ obtained after seeded-growth with different seed/monomer ratios (see also Figure S15). The L_n and L_w values increased in agreement with the feed ratio between the seed to the monomeric **4**$_{Zn}$ (for 1:1 and 1:5 seed-to-monomer ratios, L_n = 177 and 422 nm, L_w = 214 and 523 nm, respectively). Thus, the polydispersity indices (PDI, L_w/L_n) were as low as 1.21–1.24, indicative of controlled growth (Figure 4e). The controlled length with narrow polydispersity was retained at least for a week after the sample preparation, suggesting slow dynamic nature of our SPs. It should be noted that such a low PDI value could not be achieved without using the seed, i.e., if a toluene solution of **4**$_{Zn}$ was mixed with pure MCH in the scheme shown in Figure 4a (PDI = 1.49, Figure S16). Small ill-defined aggregates, which were most probably formed without the aid of the seed, were also observed particularly for the sample prepared at the 1:5 seed-to-monomer ratio (Figure 4d). We assert that the contribution of these aggregates to the following experiments is negligible because the absorption spectrum of the thus-obtained SP**4**$_{Zn}$ was identical to that of the SP**4**$_{Zn}$ prepared through heating/cooling process under thermodynamic control (Figure 3a, see Figure S17 for detail). It is worth noting that the mixing processes (shaking, stirring, injection, etc.) affected the PDI values, and it was necessary to optimize them as well;

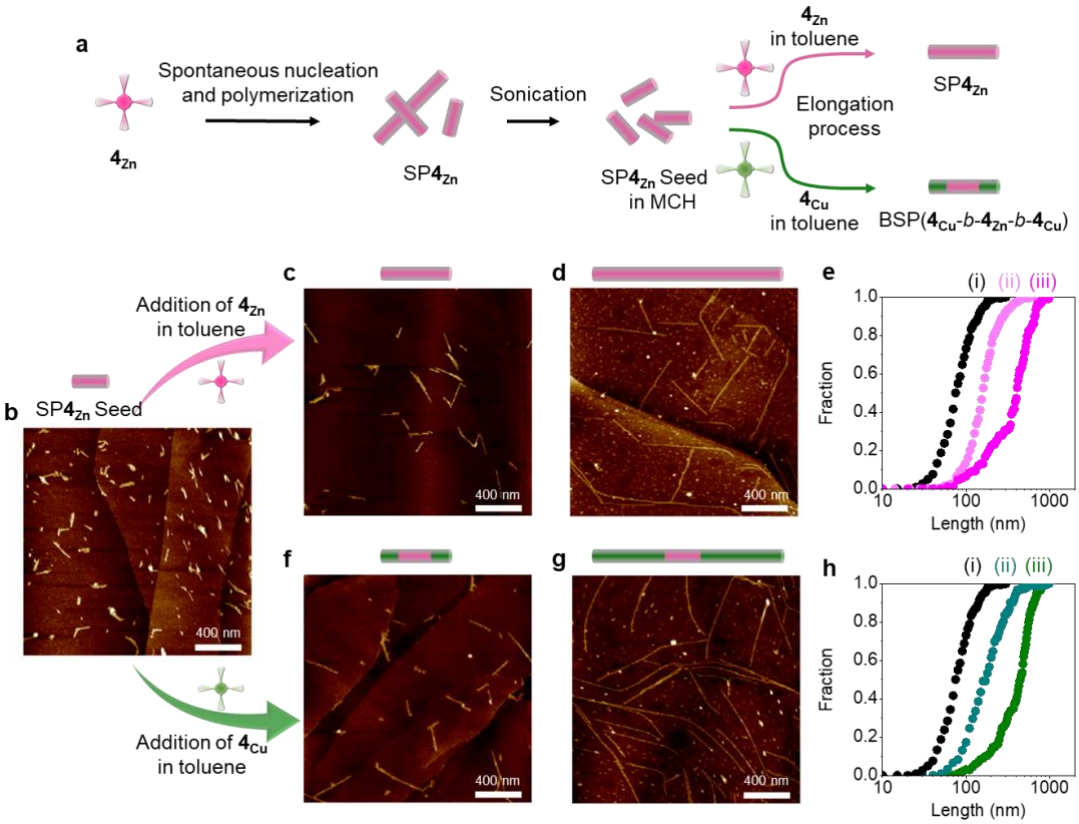

Figure 4. Living supramolecular polymerization and synthesis of block supramolecular polymers. (a) Schematic representation of living supramolecular polymerization performed via the CDSA method. (b) AFM image of seed of $SP\mathbf{4}_{Zn}$: scale bar, 400 nm. (c,d) AFM images of $SP\mathbf{4}_{Zn}$ prepared according to the scheme shown in (a): scale bar, 400 nm. The ratios between the seed of $SP\mathbf{4}_{Zn}$ and monomeric $\mathbf{4}_{Zn}$ are 1:1 (c) and 1:5 (d). (e) Cumulative histograms of the length distributions of (i) the seed of $SP\mathbf{4}_{Zn}$ and $SP\mathbf{4}_{Zn}$ prepared with the seed to monomeric $\mathbf{4}_{Zn}$ ratios of (ii) 1:1 and (iii) 1:5. (f,g) AFM images of BSP($\mathbf{4}_{Cu}$-*b*-$\mathbf{4}_{Zn}$-*b*-$\mathbf{4}_{Cu}$) prepared according to the scheme shown in **a**, scale bar = 400 nm. The ratios of the seed of $SP\mathbf{4}_{Zn}$ and monomeric $\mathbf{4}_{Cu}$ were 1:1 (f) and 1:5 (g). (h) Cumulative histograms of the length distributions of (i) the seed of $SP\mathbf{4}_{Zn}$ and BSP($\mathbf{4}_{Cu}$-*b*-$\mathbf{4}_{Zn}$-*b*-$\mathbf{4}_{Cu}$) prepared with the seed to monomeric $\mathbf{4}_{Cu}$ ratios of (ii) 1:1 and (iii) 1:5.

specifically, rapid and homogeneous mixing of the two solutions achieved lower PDI values. Further studies including the use of a variety of monomers with different structures and the combination of good/poor solvents are currently underway.

In the last decade, Manners and co-workers[34-37] have developed the living CDSA method and fabricated a variety of block nanostructures consisting of block copolymers. Fukushima, Aida, and co-workers[38] synthesized a linear heterojunction nanotubular object composed of small molecular entities (hexabenzocoronene derivatives). These seminal studies have demonstrated the unprecedented potential applications of block nanostructures. Similarly, in the scheme shown in Figure 4a, other monomers such as $\mathbf{4}_{Cu}$ in its toluene solution could be used instead of $\mathbf{4}_{Zn}$. The increased L_n and low PDI values confirmed the controlled seeded-growth, thus suggesting the formation of a block supramolecular polymer, BSP($\mathbf{4}_{Cu}$-*b*-$\mathbf{4}_{Zn}$-*b*-$\mathbf{4}_{Cu}$) (for 1:1 and 1:5 seed($SP\mathbf{4}_{Zn}$)-to-monomer($\mathbf{4}_{Cu}$) ratios, L_n = 183 and 453 nm, PDIs = 1.21 and 1.21, respectively: Figure 4f,g,h and Figure S18). Interestingly, fluorescence of $SP\mathbf{4}_{Zn}$ was quenched by block copolymerization with $SP\mathbf{4}_{Cu}$, which indicates electronic communication such as excitation energy transfer between the two blocks (Figure S19)[38,56]. The obtained BSP consisting of monomers based on distinct cores (not side chains[10,15,17]) represents a new type of multicomponent SPs[8,42-47].

Kinetic stability of the block supramolecular polymers. The reversible nature of non-covalent bonds endows SPs with unique dynamic properties such as stimuli responsiveness and self-healing ability[5-7,54] However, it also leads to a drawback that SPs are inherently unstable, hindering their further applications to a certain extent. For example, $SP\mathbf{4}_{Zn}$ was readily depolymerized in the presence of Lewis bases that coordinated to the zinc atom and prevented the porphyrin plane from forming π-stacks[55,56]. Upon the addition of 4-dimethylaminopyridine (DMAP), the H aggregate absorption band of $SP\mathbf{4}_{Zn}$ disappeared (398 nm) and a new band corresponding to DMAP-coordinated zinc(II)-porphyrin could be observed (430 nm) (Figure 5a). The Gibbs free energy for the coordination of DMAP to zinc(II)-porphyrin ($\mathbf{1}_{Zn}$) in the MCH/toluene (2/1)

mixture was determined to be –29 kJ mol^{-1} at 298 K (Figure S20), which rivaled the Gibbs free energy for the elongation of SP$_{4Zn}$ (–38 kJ mol^{-1}, see above). In contrast, SP$_{4Cu}$ was inert against DMAP because of the extremely low affinity of copper(II)-porphyrin for DMAP (Figure 5b)[57].

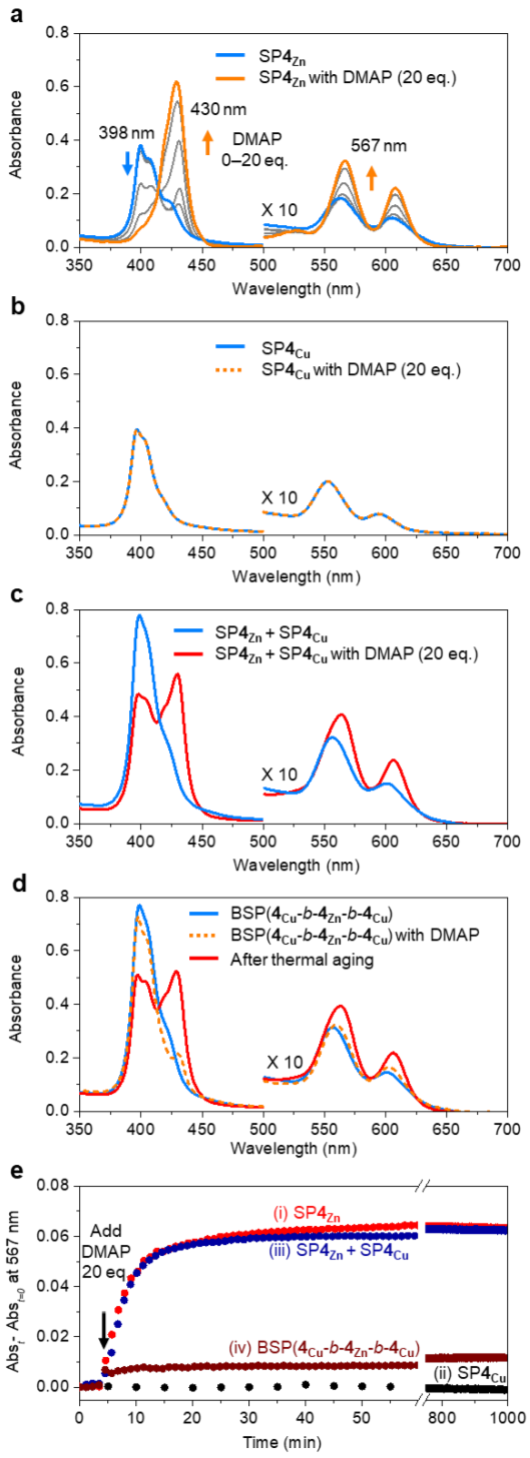

Figure 5. Kinetically enhanced stability of block supramolecular polymers. (a–d) Absorption spectra of SP$_{4Zn}$ (a), SP$_{4Cu}$ (b), a mixture of SP$_{4Zn}$ and SP$_{4Cu}$ (c), BSP(4$_{Cu}$-*b*-4$_{Zn}$-*b*-4$_{Cu}$) (d) with and without DMAP. (e) Time courses of absorbance changes because of the depolymerization of SP$_{4Zn}$ upon addition of DMAP: (i) SP$_{4Zn}$, (ii) SP$_{4Cu}$, (iii) a mixture of SP$_{4Zn}$ and SP$_{4Cu}$, and (iv) BSP(4$_{Cu}$-*b*-4$_{Zn}$-*b*-4$_{Cu}$). [4$_{Zn}$] = [4$_{Cu}$] = 10 μM and [DMAP, when added] = 200 μM, in MCH/toluene (2:1) mixed solvent.

Interestingly, the depolymerization of SP$_{4Zn}$ by DMAP was prevented in the thus-synthesized BSP(4$_{Cu}$-*b*-4$_{Zn}$-*b*-4$_{Cu}$) structure ([4$_{Zn}$] = [4$_{Cu}$] = 10 μM, Figure 5d,e and Figure S21). A small shoulder peak (430 nm) attributable to DMAP-4$_{Zn}$ complex appeared mainly due to the coexisting monomeric 4$_{Zn}$ in equilibrium (Figure 5d and see Figure S22 for detail). This result implied that the SP$_{4Cu}$ blocks at both termini shielded the SP$_{4Zu}$ block and prevented it from DMAP-triggered depolymerization. Importantly, the length histogram of the BSP(4$_{Cu}$-*b*-4$_{Zn}$-*b*-4$_{Cu}$) was retained even after the stability test (Figure S23).

For reference, the addition of DMAP to the mixture of SP$_{4Zn}$ and SP$_{4Cu}$ resulted in the selective depolymerization of SP$_{4Zn}$ (Figure 5c). Heating the solution of BSP(4$_{Cu}$-*b*-4$_{Zn}$-*b*-4$_{Cu}$) above T_e in the presence of DMAP and subsequent cooling led to a solution with an absorption spectrum identical to that obtained for the reference mixture of SP$_{4Zn}$, SP$_{4Cu}$, and DMAP (compare red lines in Figure 5c and d). In addition, application of sonication which breaks the BSP(4$_{Cu}$-*b*-4$_{Zn}$-*b*-4$_{Cu}$) thereby exposing the 4$_{Zn}$ core to the DMAP also induced the same absorption spectral change (Figure S24). These results indicate that SP$_{4Zn}$ was kinetically stabilized against the DMAP ligand in the block structure.

We could also extend random SPs composed of 4$_{Zn}$ and 4$_{Cu}$ from the seeds of SP$_{4Zn}$. Depolymerization of the segment of SP$_{4Zn}$ as an inner block was found to be stabilized against DMAP, suggesting that the blocks of random SP structure could also protect the inner SP$_{4Zn}$ (Figure S25). Previously, Schenning, Meijer, and co-workers[54,56] reported the synthesis of a random SP consisting of zinc(II)- and copper(II)-porphyrin monomers. They found that the zinc(II)-porphyrin monomer could be selectively removed from such a random SP by axial ligation with a Lewis base. A comparison of the kinetics of the system developed in the present study with Meijer's system may provide mechanistic insights into the depolymerization and monomer-exchange mechanisms.

Following previously reported methods for similar systems[58], molecular simulations was used in this study to obtain a molecular-level insight into these SPs and their DMAP-triggered depolymerization. All atom (AA) and coarse-grained (CG) models were developed for the 4$_{Zn}$ monomer (Figure 6a). The CG scheme employed in this work was consistent with that recently used for 1,3,5-benzenetricarboxamide (BTA)-based SPs, allowing us to study the SPs at a resolution of ~5 Å[59]. The AA model was used to fine-tune the CG model (see Method in Supporting Information). A pre-stacked SP model of the initially extended CG 4$_{Zn}$ monomers was equilibrated in explicit cyclohexane solvent (equivalent to MCH at the level of resolution of these CG models) via CG molecular dynamics (CG-MD) simulation[59,60] (here, we note that

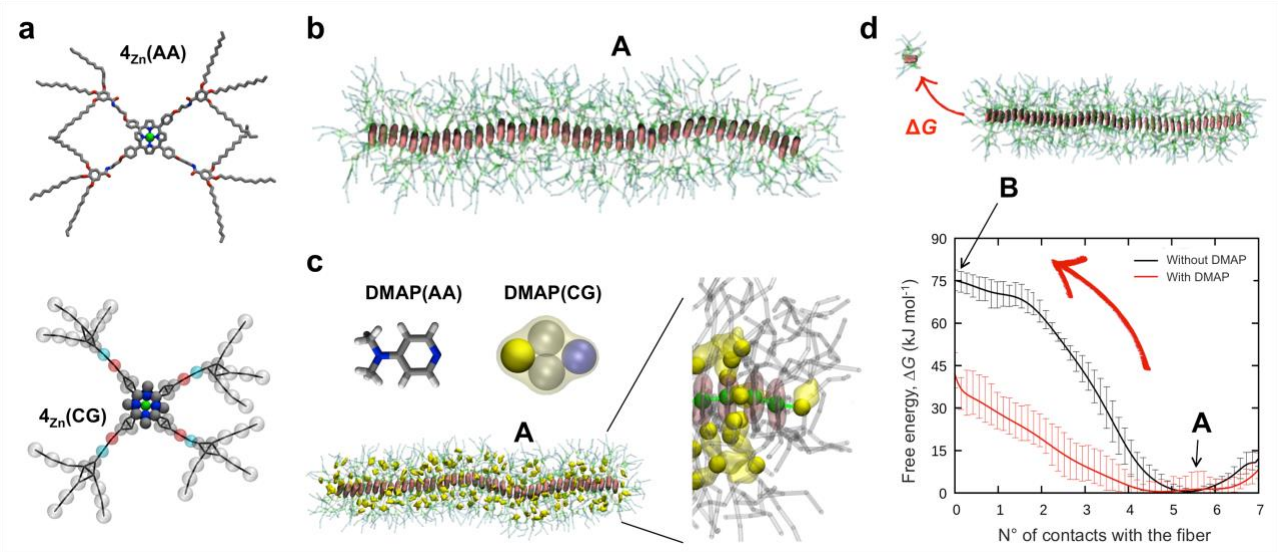

Figure 6. Molecular modeling of $\mathbf{4_{Zn}}$ supramolecular polymer. (a) Atomistic (AA) and coarse-grained (CG) models for the $\mathbf{4_{Zn}}$ monomer. (b) Equilibrated configuration of the supramolecular fiber $\mathbf{4_{Zn}(CG)}$ in cyclohexane: zinc(II)-porphyrin cores are colored in pink and the side chains are represented as grey/green transparent wires (solvent not shown for clarity). (c) AA and CG models for DMAP. Equilibrated configuration of fiber $\mathbf{4_{Zn}(CG)}$ in cyclohexane (not shown) and DMAP (yellow). Only the DMAP molecules stably absorbed/interacting with the fiber are shown. Detail: DMAP coordination to zinc (in green); stable interactions are represented as green dynamic bonds. (d) Free energy (ΔG) for monomer exchange from the fiber tips (red arrow) obtained from WT-MetaD simulations. Data are shown as a function of the number of contacts between the exchanging monomer and the rest of the fiber (state A: assembled fiber; state B: exchange) for the $\mathbf{4_{Zn}(CG)}$ fiber in cyclohexane in the absence (black) and presence of DMAP (red).

DMAP depolymerizes $SP\mathbf{4_{Zn}}$ even in pure MCH). An equilibrated configuration of $SP\mathbf{4_{Zn}}$ was obtained, which appeared as a very stable, extended fiber of unimolecular width under these conditions (Figure 6b). Next, explicit CG DMAP molecules were inserted in the simulation box with a DMAP:$\mathbf{4_{Zn}}$ ratio of 20:1, and the system was re-equilibrated. It was observed that the DMAP molecules were adsorbed onto the surface of $SP\mathbf{4_{Zn}}$ without being able to access the zinc atoms in the interior of $SP\mathbf{4_{Zn}}$. As shown in Figure 6c, it was only at the fiber tips that the DMAP molecules were stably coordinated to the porphyrin zinc atoms.

Next, the effect of DMAP on the depolymerization of $SP\mathbf{4_{Zn}}$ was investigated. Following the recently reported method to study the dynamics of BTA-based SPs,[61] well-tempered metadynamics (WT-MetaD)[62] simulation was used to activate and explore the monomer exchange process (see Method in Supporting Information). In the native condition (without DMAP), the global free energy difference between the assembled (**A**: N+1 assembled monomers) and disassembled state (**B**: N assembled + 1 disassembled) was found to be ~65 kJ mol^{-1} (Figure S26). This value is in reasonable agreement with the experimentally determined ΔG for the elongation of $SP\mathbf{4_{Zn}}$ in MCH (52 kJ mol^{-1}, Figure S8). In the monomer exchange process from the $SP\mathbf{4_{Zn}}$ tips, the system had to overcome a free energy barrier of ~75 kJ mol^{-1} (Figure 6d, black). We also investigated monomer exchange process from the middle of $SP\mathbf{4_{Zn}}$ via WT-MetaD simulations. In this mechanism, the $SP\mathbf{4_{Zn}}$ first broke down to form a defect or a new tip (Step 1: ΔG_1 = ~70 kJ mol^{-1} needed), from which the monomer could then exchange (Step 2: see above): a mechanism also observed in BTA-based SPs in an organic solvent[61]. Assuming (underestimating) steps 1 and 2 as simply additive, and given the exponential relationship between the free energy barriers to cross and the characteristic probability for the events to occur, we can conclude that the monomer exchanges occurs predominantly from the fiber tips.

Interestingly, the same analysis on $SP\mathbf{4_{Zn}}$ in the presence of DMAP demonstrated that the free energy barrier for monomer exchange from the fiber tip decreased to ~40 kJ mol^{-1} (Figure 6d, red). Thus, free energy of the process was reduced by ~35 kJ mol^{-1} when compared to the same SP in the absence of DMAP, which was in agreement with the competing DMAP-zinc experimental affinity in MCH (~30 kJ mol^{-1}: see, Figure S20). The free energy profile of monomer dissociation from the fiber tip obtained from WT-MetaD under such out-of-equilibrium conditions demonstrated that the DMAP molecules interfered with the monomer–monomer interactions at the fiber tip, first by penetrating in between the porphyrin cores and then by facilitating monomer detachment from the fiber tip (Figure S27). These results corroborate the stabilization scheme for BSPs demonstrated above, where $SP\mathbf{4_{Cu}}$ blocks at both tips of the $SP\mathbf{4_{Zn}}$ block could prevent $SP\mathbf{4_{Zn}}$ from DMAP-triggered depolymerization, by saturating the *de facto* depolymerization "hot spots" (i.e., the $SP\mathbf{4_{Zn}}$ tips). A similar strategy to enhance the stability of SP—one based

on the mechanism in which monomer exchange hot spots are decreased—has recently been reported by Palmans, Meijer, and co-workers[63] for supramolecular copolymers, but to the best of our knowledge, this is the first example demonstrated by using BSPs.

CONCLUSIONS

The concept of living supramolecular polymerization has rapidly evolved in recent years[3,4,9-25]; nevertheless, the synthesis of BSPs still remains a challenge. As discussed at the beginning of this article, the dilemma of molecular design for connecting two distinct SPs needs to be addressed. Herein, it was demonstrated that BSPs could be synthesized in a similar manner as the living CDSA method[16,17,34-37]. Although the conditions of seeded growth remain to be explored from the viewpoint of kinetics, the controlled length of the thus-obtained BSPs with narrow polydispersity confirmed that supramolecular polymerization occurred in the seeded growth mechanism.

It is noteworthy that $SP_{\mathbf{4}_{Zn}}$, as an inner block in the BSP ($\mathbf{4}_{Cu}$-*b*-$\mathbf{4}_{Zn}$-*b*-$\mathbf{4}_{Cu}$), could coexist with DMAP that was otherwise incompatible with $SP_{\mathbf{4}_{Zn}}$ alone. Thus, it appears that a SP can be kinetically *compartmentalized* in the block structure. As illustrated in many biomolecular systems, compartmentalization is a key concept for achieving intricate multicomponent systems. The present finding can lead to many opportunities for the design of unprecedented functional supramolecular systems; in this context, for example, DMAP is a well-known organic catalyst and may function as such in the BSP matrix. Obviously, an emergence of unique properties from the combination and sequence of the blocks can also be expected[64]. We believe that the synthetic strategy and characterization of BSPs demonstrated in this work will contribute to a better understanding of their attributes and applications for the development of multicomponent supramolecular systems.

ASSOCIATED CONTENT

Supporting Information. Experimental details, AFM images, spectroscopic data. "This material is available free of charge via the Internet at http://pubs.acs.org."

AUTHOR INFORMATION

Corresponding Author

* giovanni.pavan@supsi.ch (G.M.P.),
*TAKEUCHI.Masayuki@nims.go.jp (M.T.),
*SUGIYASU.Kazunori@nims.go.jp (K.S.)

Notes

The authors declare no competing financial interest.

ACKNOWLEDGMENT

This work was supported by KAKENHI (JP15H05483 for K.S.), Scientific Research on Innovative Arias "Dynamical ordering of biomolecular systems for creation of integrated functions (JP16H00787)", "π-System figuration: control of electron and structural dynamism for innovative functions (JP26102009 for M.T.)", and the Nanotechnology Network Project from the Ministry of Education, Culture, Sports, Science and Technology, Japan. S.H.J. thanks the Japan Society for the Promotion of Science (JSPS) for a postdoctoral fellowship for overseas researchers (16F16043). D.B. and G.M.P. acknowledge the Swiss National Science Foundation (SNSF grant 200021_175735 to G.M.P.).

REFERENCES

1. Odian, G. *Principles of polymerization*, fourth edition; A John Wiley & Sons, Inc., Publication, Hoboken, New Jersey, 2004
2. Lutz, J.-F.; Lehn, J.-M.; Meijer, E. W.; Matyjaszewski, K. From precision polymers to complex materials and systems. *Nat. Rev. Mater.* **2016**, *1*, 16024.
3. Vanderzwaag, D.; DeGreef, T. F. A.; Meijer, E. W. Programmable supramolecular polymerizations. *Angew. Chem. Int. Ed.* **2015**, *54*, 8334.
4. Mukhopadhyay, R. D.; Ajayaghosh, A. Living supramolecular polymerization. *Science* **2015**, *349*, 241-242.
5. Aida, T.; Meijer, E. W.; Stupp, S. I. Functional supramolecular polymers. *Science* **2012**, *335*, 813–817.
6. Webber, M. J.; Appel, E. A.; Meijer, E. W.; Langer, R. Supramolecular biomaterials. *Nat. Mater.* **2015**, *15*, 13–26.
7. Yang, L.; Tan, X.; Wang, Z.; Zhang, X. Supramolecular polymers: historical development, preparation, characterization, and functions. *Chem. Rev.* **2015**, *115*, 7196–7239.
8. Adelizzi, B., Aloi, A.; Markvoort, A. J.; Ten Eikelder, H. M. M.; Voets, I. K.; Palmans, A. R. A.; Meijer, E. W. Supramolecular block copolymers under thermodynamic control. *J. Am. Chem. Soc.* **2018**, *140*, 7168–7175.
9. Ogi, S.; Sugiyasu, K.; Manna, S.; Samitsu, S.; Takeuchi, M. Living supramolecular polymerization realized through a biomimetic approach. *Nat. Chem.* **2014**, *6*, 188–195.
10. Fukui, T.; Kawai, S.; Fujinuma, S.; Matsushita, Y.; Yasuda, T.; Sakurai, T.; Seki, S.; Takeuchi, M.; Sugiyasu, K. Control over differentiation of a metastable supramolecular assembly in one and two dimensions. *Nat. Chem.* **2017**, *9*, 493-499.
11. Kang, J.; Miyajima, D.; Mori, T.; Inoue, Y.; Itoh, Y.; Aida, T. A rational strategy for the realization of chain-growth supramolecular polymerization. *Science* **2015**, *347*, 646–651.
12. Ogi, S.; Stepanenko, V.; Sugiyasu, K.; Takeuchi, M.; Würthner, F. Mechanism of self-assembly process and seeded supramolecular polymerization of perylene bisimide organogelator. *J. Am. Chem. Soc.* **2015**, *137*, 3300–3307.
13. Ogi, S.; Stepanenko, V.; Thein, J.; Würthner, F. Impact of alkyl spacer length on aggregation pathways in kinetically controlled supramolecular polymerization. *J. Am. Chem. Soc.* **2016**, *138*, 670–678.
14. Wagner, W.; Wehner, M.; Stepanenko, V.; Ogi, S.; Würthner, F. Living supramolecular polymerization of a perylene bisimide Dye into fluorescent J-aggregates. *Angew. Chem. Int. Ed.* **2017**, *56*, 16008–16012.
15. Pal, A.; Malakoutikhah, M.; Leonetti, G.; Tezcan, M.; Colomb-Delsuc, M.; Nguyen, V. D.; van der Gucht, J.; Otto, S. Controlling the structure and length of self-synthesizing supramolecular polymers through nucleated growth and disassembly. *Angew. Chem. Int. Ed.* **2015**, *54*, 7852-7856.
16. Robinson, M. E.; Lunn, D. J.; Nazemi, A.; Whittell, G. R.; De Cola, L.; Manners, I. Length control of supramolecular polymeric nanofibers based on stacked planar platinum(II) complexes by seeded-growth. *Chem. Commun.* **2015**, *51*, 15921-15924.
17. Robinson, M. E.; Nazemi, A.; Lunn, D. J.; Hayward, D. W.; Boott, C. E.; Hsiao, M.-S.; Harniman, R. L.; Davis, S. A.; Whittell, G. R.; Richardson, R. M.; De Cola, L.; Manners, I.

Dimensional control and morphological transformations of supramolecular polymeric nanofibers based on cofacially-stacked planar amphiphilic platinum(II) complexes. *ACS Nano* **2017**, *11*, 9162-9175.
18. Haedler, A. T.; Meskers, S. C. J.; Zha, R. H.; Kivala, M.; Schmidt, H. W.; Meijer, E. W. Pathway complexity in the enantioselective self-assembly of functional carbonyl-bridged triarylamine trisamides. *J. Am. Chem. Soc.* **2016**, *138*, 10539-10545.
19. Endo, M.; Fukui, T.; Jung, S. H.; Yagai, S.; Takeuchi, M.; Sugiyasu, K. Photoregulated living supramolecular polymerization established by combining energy landscapes of photoisomerization and nucleation-elongation processes. *J. Am. Chem. Soc.* **2016**, *138*, 14347-14353.
20. Ogi, S.; Matsumoto, K.; Yamaguchi, S. Seeded polymerization through the interplay of folding and aggregation of an amino-acid-based diamide. *Angew. Chem. Int. Ed.* **2018**, *57*, 2339–2343.
21. Greciano, E. E.; Matarranz, B.; Sanchez, L. Pathway complexity versus hierarchical self-assembly in N-annulated perylenes. Structural effects in seeded supramolecular polymerization. *Angew. Chem. Int. Ed.* **2018**, *57*, 4697-4701.
22. Mishra, A.; Korlepara, D. B.; Kumar, M.; Jain, A.; Jonnalagadda, N.; Bejagam, K. K.; Balasubramanian, S.; George, S. J. Biomimetic temporal self-assembly via fuel-driven controlled supramolecular polymerization. *Nat. Commun.* **2018**, *9* , 1295.
23. Ghosh, G.; Ghosh, S. Solvent dependent pathway complexity and seeded supramolecular polymerization. *Chem. Commun.*, **2018**, *54*, 5720-5723.
24. Sorrenti, A.; Leira-Iglesias, J.; Markvoort, A. J.; de Greef, T. F. A.; Hermans, T. M. Non-equilibrium supramolecular polymerization. *Chem. Soc. Rev.*, **2017**, 46, 5476-5490.
25. Dhiman, S.; George, S. J. Temporally controlled supramolecular polymerization. *Bull. Chem. Soc. Jpn*. **2018**, 91, 687–699.
26. De Greef, F.A.; Smulders, M.J.; Wolffs, M.; Schenning, A.P.H.J.; Sijbesma, R.P.; Meijers, E. W. Supramolecular polymerization. *Chem. Rev.* **2009**, *109*, 5687–5754.
27. Zhao, D.; Moore, J. S. Nucleation-elongation: a mechanism for cooperative supramolecular polymerization. *Org. Biomol. Chem.* **2003**, *1*, 3471–3491.
28. Chen, Z.; Lohr, A.; Saha-Möller, C. R.; Würthner, F. Self-assembled π-stacks of functional dyes in solution: structural and thermodynamic features. *Chem. Soc. Rev.* **2009**, *38*, 564–584.
29. Rest, C.; Kandanelli, R.; Fernández, G. Strategies to create hierarchical self-assembled structure *via* cooperative non-covalent interactions. *Chem. Soc. Rev.* **2015**, *44*, 2543–2572.
30. Adolf, C. R. R.; Ferlay, S.; Kyritsakas, N.; Hosseini, M. W. Welding molecular crystals *J. Am. Chem. Soc.* **2015**, *137*, 15390–15393.
31. Ogi, S.; Fukui, T.; Jue, M. L.; Takeuchi, M.; Sugiyasu, K. Kinetic control over pathway complexity in supramolecular polymerization through modulating the energy landscape by rational molecular design. *Angew. Chem. Int. Ed.* **2014**, 53, 14363–14367.
32. Nicewarner-Peña, S. R.; Freeman, R. G.; Reiss, B. D.; He, L.; Peña, D. J.; Walton, I. D.; Cromer, R.; Keating, C. D.; Natan, M. J. Submicrometer metallic barcodes. *Science* **2001**, *294*, 137-141.
33. Park, S.; Lim, J.-H.; Chung, S.-W.; Mirkin, C. A. Self-assembly of mesoscopic metal-polymer amphiphiles. *Science* **2004**, *303*, 348–351.
34. Wang, X.; Guerin, G.; Wang, H.; Wang, Y.; Manners, I.; Winnik, M. Cylindrical block copolymer micelles and co-micelles of controlled length and architecture. *Science* **2007**, *317*, 644-648.
35. Gilroy, J. B.; Gädt, T.; Whittell, G. R.; Chabanne, L.; Mitchels, J. M.; Richardson, R. M.; Winnik, M. A.; Manners, I. Monodisperse cylindrical micelles by crystallization-driven living self-assembly. *Nat. Chem.* **2010**, *2*, 566-570.
36. Rupar, P. A., Chabanne, L., Winnik, M. A. & Manners, I. Non-centrosymmetric cylindrical micelles by unidirectional growth. *Science* **337**, 559–562 (2012).
37. Hudson, Z. M.; Lunn, D. J.; Winnik, M. A.; Manners, I. Colour-tunable fluorescent multiblock micelles. *Nat. Commun.* **2014**, 5, 3372.
38. Zhang, W.; Jin, W.; Fukushima, T.; Saeki, A.; Seki, S.; Aida, T. Supramolecular linear heterojunction composed of graphite-like semiconducting nanotubular segments. *Science* **2011**, *334*, 340-343.
39. Beun, L. H.; Albertazzi, L.; van der Zwaag, D.; de Vries, R.; Stuart, M. A. C. Unidirectional living growth of self-assembled protein nanofibrils revealed by suprer-resolution microscopy. *ASC Nano* **2016**, *10*, 4973–4980.
40. Zhang, K.; Yeung, M. C.-L.; Leung, S. Y.-L.; Yam, V. W.-W. Living supramolecular polymerization achieved by collaborative assembly of platinum(II) complexes and block copolymers. *Proc. Natl. Acad. Sci.* **2017**, *114*, 11844–11849.
41. Korevaar, P. A.; Schaefer, C.; de Greef, T. F. A.; Meijer, E. W. Controlling chemical self-assembly by solvent-dependent dynamics. *J. Am. Chem. Soc.* **2012**, *134*, 13482–13491.
42. Besenius, P. Controlling supramolecular polymerization through multicomponent self-assembly. *J. Polym. Sci. A* **2017**, 55, 34-78.
43. Yagai, S. Supramolecularly engineered functional π-assemblies based on complementary hydrogen-bonding interactions. *Bull. Chem. Soc. Jpn.* **2014,** *88*, 28-58.
44. Görl, D., Zhang, X.; Stepanenko, V.;Würthner, F. Supramolecular block copolymers by kinetically controlled co-self-assembly of planar and core-twisted perylene bisimides. *Nat. Commun.* **2015**, *6*, 7009.
45. Hirao, T.; Kudo, H., Amimoto, T.; Haino, T. Sequence-controlled supramolecular terpolymerization directed by specific molecular recognitions. *Nat. Commun.* **2017**, *8*, 634.
46. Qin, B.; Zhang, S.; Song, Q.; Huang, Z.; Xu, J. F.; Zhang, X. Supramolecular interfacial polymerization: a controllable method of fabricating supramolecular polymeric materials. *Angew. Chem. Int. Ed.* **2017**, *56*, 7639-7643.
47. Miyauchi, M.; Harada, A. Construction of supramolecular polymers with alternating α-, β-cyclodextrin units using conformational change induced by competitive guest. *J. Am. Chem. Soc.* **2004**, *126*, 11418–11419.
48. Valicsek, Z.; Horváth, O. Application of the electronic spectra of porphyrins for analytical purposes: The effects of metal ions and structural distortions. *Microchem. J.* **2013**, *107*, 47–62.
49. Mabesoone, M. F. J.; Markvoort, A. J.; Banno, M.; Yamaguchi, T.; Helmich, F.; Naito, Y.; Yashima, E.; Palmans, A. R. A.; Meijer, E. W. Competing interaction in hierarchical porphyrin self-assembly introduce robustness in pathway complexity. *J. Am. Chem. Soc.* **2018**, *140*, 7810–7819
50. Hifsudheen, M.; Mishra, R. K.; Vedhanarayanan, B.; Praveen, V. K.; Ajayaghosh, A. The helix to super-helix transition in the self-assembly of π-systems: superseding of molecular chirality at hierarchical level. *Angew. Chem., Int. Ed.* **2017**, 56, 12634–12638.
51. Jonkheijm, P.; van der Schoot, P.; Schenning, A. P. H. J.; Meijer, E. W. Probing the solvent-assisted nucleation pathway in chemical self-assembly. *Science* **2006**, *313*, 80–83.

52. Smulders, M. M. J.; Schenning, A. P. H. J.; Meijer, E. W. Insight into the mechanisms of cooperative self-assembly: the 'sergeants-and-soldiers' principle of chiral and achiral C_3-symmetrical discotic triamides. *J. Am. Chem. Soc.* **2008**, *130*, 606–611.
53. Smulders, M. M. J.; Nieuwenhuizen, M. M. L.; Greef, T. F. A.; Schoot, P.; Schenning, A. P. H. J.; Meijer, E. W. How to Distinguish isodesmic from cooperative supramolecular polymerisation. *Chem. Eur. J.* **2010**, *16*, 362-367.
54. Torchi, A.; Bochicchio, D.; Pavan, G. M. How the dynamics of a supramolecular polymer determines its dynamic adaptivity and stimuli-responsiveness: structure-dynamics-property relationships from coarse-grained simulations. *J. Phys. Chem. B* **2018**, *122*, 4169-4178.
55. Helmich, F.; Lee, C. C., Schenning, A. P. H. J.; Meijer, E. W. Chiral memory via chiral amplification and selective depolymerization of porphyrin aggregates. *J. Am. Chem. Soc.* **2010**, *132*, 16753–16755.
56. Helmich, F.; Smulders, M. M. J.; Lee, C. C.; Schenning, A. P. H. J.; Meijer, E. W. Effect of stereogenic centers on the self-sorting, depolymerization, and atropisomerization kinetics of porphyrin-based aggregates. *J. Am. Chem. Soc.* **2011**, *133*, 12238–12246.
57. Cremers, J.; Richert, S.; Kondratuk, D. V.; Claridge, T. D. W.; Timmel, C. R.; Anderson, H. L. Nanorings with copper(II) and zinc(II) centers: forcing copper porphyins to bind axial ligands in heterometallated oligomers. *Chem. Sci.* **2016**, *7*, 6961-6968.
58. Bochicchio, D.; Pavan, G. M. Molecular modeling of supramolecular polymers. *Adv. Phys. X* **2018**, *3*, 1436408.
59. Bochicchio, D.; Pavan, G. M. From cooperative self-assembly to water-soluble supramolecular polymers using coarse-grained simulations. *ACS Nano* **2017**, *11*, 1000–1011.
60. Garzoni, M.; Baker, M. B.; Leenders, C. M. A.; Voets, I. K.; Albertazzi, L.; Palmans, A. R. A.; Meijer, E. W.; Pavan, G. M. Effect of H-bonding on order amplification in the growth of a supramolecular polymer in water. *J. Am. Chem. Soc.* **2016**, *138*, 13985-13995.
61. Bochicchio, D.; Salvalaglio, M.; Pavan, G. M. Into the dynamics of a supramolecular polymer at submolecular resolution. *Nat. Commun.* **2017**, 8, 147.
62. Barducci, A.; Bussi, G.; Parrinello, M. Well-tempered metadynamics: a smoothly converging and tunable free-energy method. *Phys. Rev. Lett.* **2008**, *100*, 020603.
63. Thota, B. N. S.; Lou, X.; Bochicchio, D.; Paffen, T. F. E.; Lafleur, R. P. M.; van Dongen, J. L. J.; Ehrmann, S.; Haag, R.; Pavan, G. M.; Palmans, A. R. A.; Meijer, E. W. *Angew. Chem. Int. Ed.* **2018**, 57, 6843–6847.
64. Schacher, F. H.; Rupar, P. A.; Manners, I. Functional block copolymers: nanostructured materials with emerging applications. *Angew. Chem. Int. Ed.* **2012**, *51*, 7898–7921.

SYNOPSIS TOC

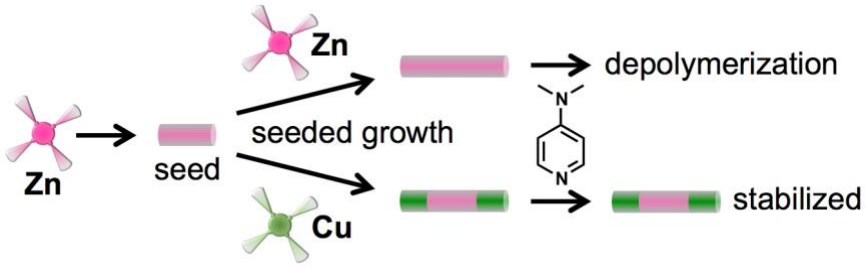
Zn
Zn
seed
seeded growth
Cu
depolymerization
N
N
stabilized